ACOUSTIC EMISSION DIAGNOSTICS OF HAZARDOUS DYNAMIC DAMAGES: CRACKING, LEAKAGE, IMPACT.

T.B. PETERSEN, V.V. SHEMYAKIN DIAPAC Ltd., 1-st Pechotny per. 6, Moscow, RUSSIA

1. Introduction

Depending on the frequency range used by passive acoustic methods of nondestructive testing these methods may be conventionally divided into three categories: low frequency, the range 0.5Hz – 10 kHz (vibrations and loose part detection); middle frequency, 2 kHz-20 kHz (leakage monitoring); high frequency, 10 kHz – 1MHz (acoustic emission).

Due to fast sporadic character of fracturing process acoustic waves caused by initiation and growth of cracks have wide spectrum. It means that this kind of damaging can be successfully inspected by means of acoustic emission method. The impacts, which also constitute a danger to the structural integrity of material, however, have relatively low spectrums, much lower than the frequency range of AE method. That is why stress waves from impact are monitored by a low frequency acoustic technique, while in AE monitoring the impact signals are regarded as acoustic interferences, which have to be rejected from the useful AE data. A leakage in turn is a continuous not a sporadic process, which is traditionally controlled by an acoustic leakage detection method.

The goal of the paper is to demonstrate the abilities and perspectives of AE technique for monitoring all mentioned sources related to dangerous damages regardless of the nature and spectral features of these sources. The paper sums up numerous results obtained by authors in the fields of acoustic emission phenomena, fracture mechanics and nondestructive testing. The research includes the development of different analytical, numerical and experimental methods for specifying types and parameters of examined AE sources.

2. AE from impacts

Mechanical parameters of colliding bodies and stress distribution in the contact zone are usually analyzed by means of so called Hertz's theory of impact. The theory gives a force-deformation relation needed to estimate the duration of impact and the maximum indentation for spheroidal surfaces, which is also valid for any 3D non-conformal contact of solids, under the condition that the contact area remains small compared to the bodies' dimensions. A detailed coverage of the theory was given by Johnson [1] and Goldsmith [2].

Derived on the basis of the Hertz law, a solution for the maximum indentation h_{ma} and contact time T of elastic impact of a sphere on a smooth surface of rigid massive plate is given by formula:

$$h_m = \left(\frac{15}{16} m v_0^{\,2} (x_1 + x_2) R^{-0.5} \right)^{0.4}, \qquad (1)$$

where

$$x_i = \frac{(1 - \upsilon_i^{\,2})}{E_i}$$

$$T = 2.9432 \cdot \left(\frac{15}{16} (x_1 + x_2) \right)^{0.4} m^{0.4} v_0^{\,-0.2} R^{-0.2}. \qquad (2)$$

Here h_m – is maximum displacement of the bodies, i.e. total of deformation of both surfaces, v_0 – is a sphere velocity at a moment of collision, R is a sphere radius, m - is a sphere mass, $E_{1(2)}$ and $\upsilon_{1(2)}$ are Young's modulus and Poisson's ratio for the plate (sphere), respectively. The formula was obtained on the assumption that m<<M, where M is a plate mass.

A phenomenon of stress wave generation occurring at impact was applied by Goldsmith [2] and also covered by Zukas *et al*. [3]. The results were obtained on assumption that stress wave effects account for a small fraction of impact energy and do not influence the local deformation significantly.

A temporal dependence of surface displacement in a top point of a sphere was first derived by Deresiewicz [4] in a form of a half-sine function, describing the dependence with high precision:

$$h(t) = h_m \sin(\frac{\pi\ t}{T}) \tag{3}$$

Frequency range of impact disturbance can be estimated from (3) in a standard way on assumption that the main impact energy lies in the range between zero and the frequency value, at which the spectrum S_w of the displacement function vanishes for the first time. Fourier transform of a half-sine is calculated by the formula:

$$S_\omega = \frac{2h_m T}{\pi} \cdot \frac{\cos(\omega \frac{T}{2})}{1 - \left(\frac{2}{\pi}\omega\frac{T}{2}\right)^2}. \tag{4}$$

This function gives a first zero at $\omega\frac{T}{2} = \frac{3}{2}\pi$, from which the desired frequency range is calculated as $\Delta f = \frac{3}{2T}$. As expected, the frequency range and the contact time are related inversely, meaning the shorter is a contact time, i.e. the less is a mass and the higher is a velocity of a body, the broader is an impact spectrum.

Here the physical variable h(t), which is a mechanic disturbance is yet not a stress wave itself – waves are generated at moments corresponding to discontinuities of the perturbation function. The lower is the order and the higher is the value of the discontinuity, the higher is the amplitude of the wave front, i.e. the amplitude of AE signal. While the surface deformation h(t) is a continuous function, its first derivative, which is a displacement velocity has two ordinary discontinuities at the initial and the final moments of the impact contact time. Besides, the high frequency tract is known to be more sensitive to derivative of the function, than to the function itself. It means that impact should produce two high frequency wave fronts, arriving with delay equal to the contact period.

From (3) a difference of the function derivative limits in the points of discontinuity, i.e a velocity jump value (discontinuity value), hence a signal amplitude may be obtained in a form of:

$$A \propto \Delta v = \pm\frac{\pi h_m}{T}, \tag{5}$$

2.1 Output AE signals analysis

To analyze the AE waveforms from impacts, a numerical modeling of collisions of a metal sphere (R = 11 mm) dropped upon a thick duralumin plate from the height of 0.3 m with a zero initial velocity was carried out. R50I transducer (PAC production) response was used at modeling to calculate output AE signal from impact.

An input source function, h(t), given in fig 1.b was calculated using the formulas (1-4) in a form of half-sine. A response of the plate – transducer - AE system on Shu-Nielsen pencil lead breaking, presented in fig.1a, was assumed a pulse characteristic of the system, $p_{sys}(t)$.

A convolution of the pulse characteristic of the system with the input source function $s(t) = h(t) * p_{sys}(t)$, given in fig.1c demonstrates the presence of low frequency, which was

removed from the final high frequency output signal by passing s(t) through a high-pass 5-th order Butterworth filter with a cutoff frequency of 50 kHz. The result of the processing is shown in fig 1d, where one can easily distinguish two separate signals coming with a delay equal to the impact duration.

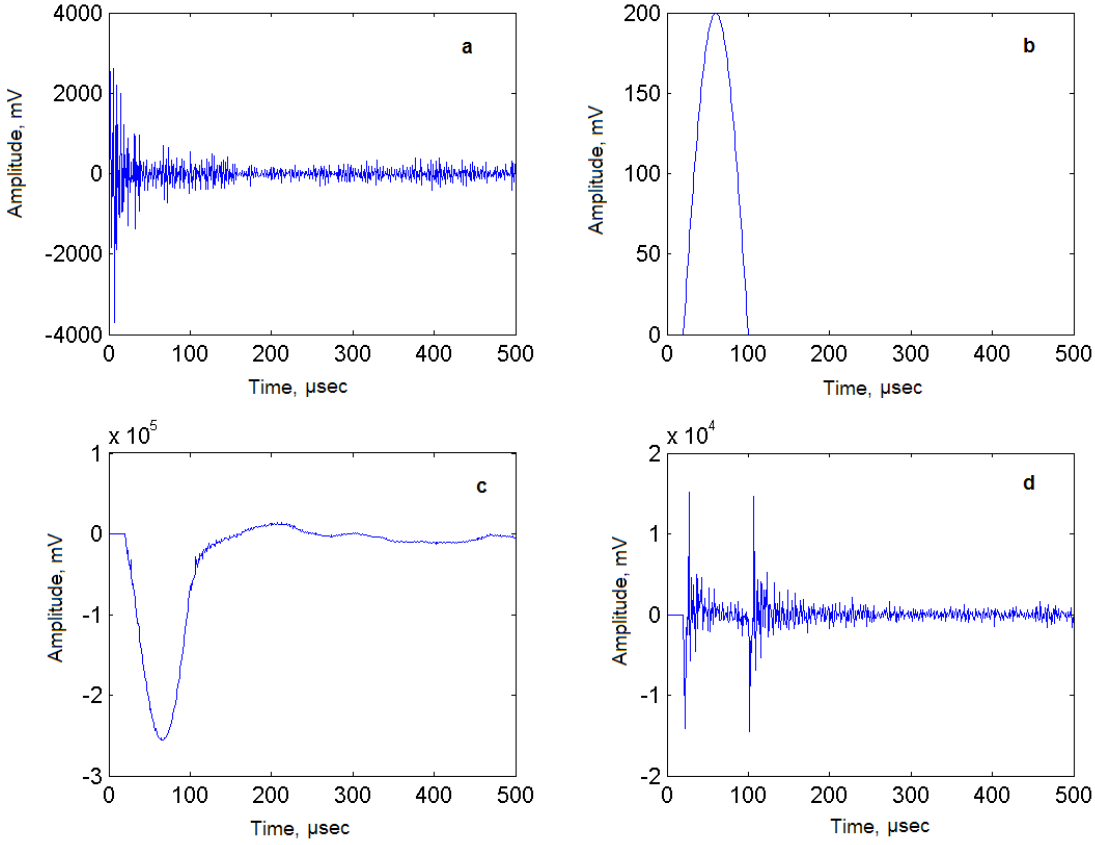

Figure 1. Modeling of a high frequency impact response a) p_{sys} -system pulse response; b) h(t) - half-sine input function; c) the convolution of (a) and (b); the output high frequency signal.

Analysis shows that a pair of signals occur when the cutoff frequency of the high-pass filter have the same or a higher order than the highest frequency of impact, determined from (4). If the impact duration, T, and the sensor decay constant, τ, satisfy the condition of $T >> \tau$, the signals do not overlap and are separated in a time domain by a delay equal to impact duration.

2.2 Experimental setup and results

Normal collisions of steel spheres dropped upon the plate surface from three different heights (100 mm, 2 mm and 300 mm) with a zero initial velocity served as AE sources. Recoil heights were registered for impact energy loss analysis.Three different sizes of spheres were used, with radius ranging from 3.5 mm to 11 mm. Experimental setup consisted of a horizontal duralumin plate having size 300x495x95 mm^3 , DiSP system and R50I AE transducer mounted on the same surface with the sphere impact location at the distance of 20 mm from the source.

The data given in table 1 were obtained at a height of falling H= 0.3 m and include both geometrical and mechanical parameters of the spheres and the corresponding characteristics of impacts, such as contact time, maximum impact surface displacement and maximum frequency calculated in accordance with formulas (1-4).

Table 1 Mechanical parameters of dropping spheres and impacts

Sphere radius, R, mm	Max indentation ,h_m (calc), mm	Impact duration, T (calc), μsec	Impact frequency, F (calc), kHz	Impact duration, <T> (exp), μsec	Standard deviation, σ (exp), μsec
11	0.069	84	9	82,8	1.03
8	0.050	61.1	12	61,4	0.4
3.5	0.022	26.7	28	28,4	0.9

The initial velocities of the spheres at impacts calculated as $v = \sqrt{2gH}$ were equal to 2.42 m/sec, here g is acceleration of gravity. Note that the same velocity value is given by the formula (5).

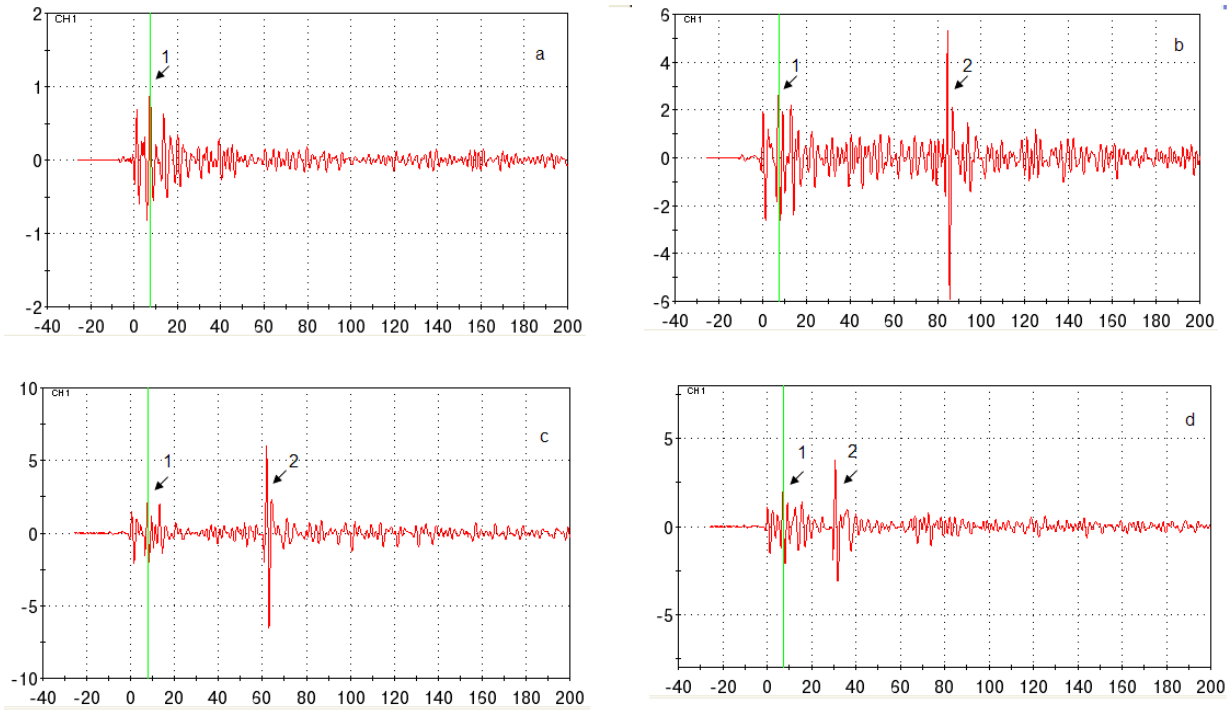

Figure 2. AE measurements conducted at the duralumin plate: (a) Shu-Nielsen pen breaking related waveform; (b-d) AE signals registered from impacts of different size spheres (with the radius of 11 mm; 8 mm; 3.5 mm, respectively) dropped upon the plate.

A restitution coefficient, *e*, which is a measure of an energy loss during impact was estimated as a quotient $e = v_f/v_i$, where v_i and v_f are velocities before and after impact, respectively. The coefficient changed from 0.61 for the large sphere (R=11 mm) to 0.7 for the small one (R = 2.5 mm) indicating the presence of energy dissipation during the impact experiments. Dissipation mechanisms observed are both plastic deformation of the plate and wave emission, which is confirmed by the presence of shallow indentations at the surface of the plate remaining after the collisions and a stress wave emission during impacts.

The examples of typical impact waveforms recorded for every sphere size are given in fig. 2b-d. For more comprehensive analysis a Shu-Nielsen pencil lead breaking response, which is considered as an impulse response of the whole system (plate - transducer-AE apparatus) at a distance of 20mm from the source is plotted in fig.2a.

Measured values of first peak amplitudes (marked by arrow #1) for all sphere sizes approximate to 2 V (86 dB). Practically independence of AE amplitudes from the sphere size may serve as experimental validation of the statement (see formula 5) that at high frequencies the first peak amplitude corresponds to the initial loading velocity (equal to 2.42 m/sec). This conclusion is also confirmed by the good correlation between the velocities obtained for three different heights of dropping spheres and the corresponding loading related amplitudes of the AE waveforms. A-V dependence shown in fig.3 is fitted by linear function $A = 1.1V - 0.38$ with the correlation coefficient $R_c = 0.85$.

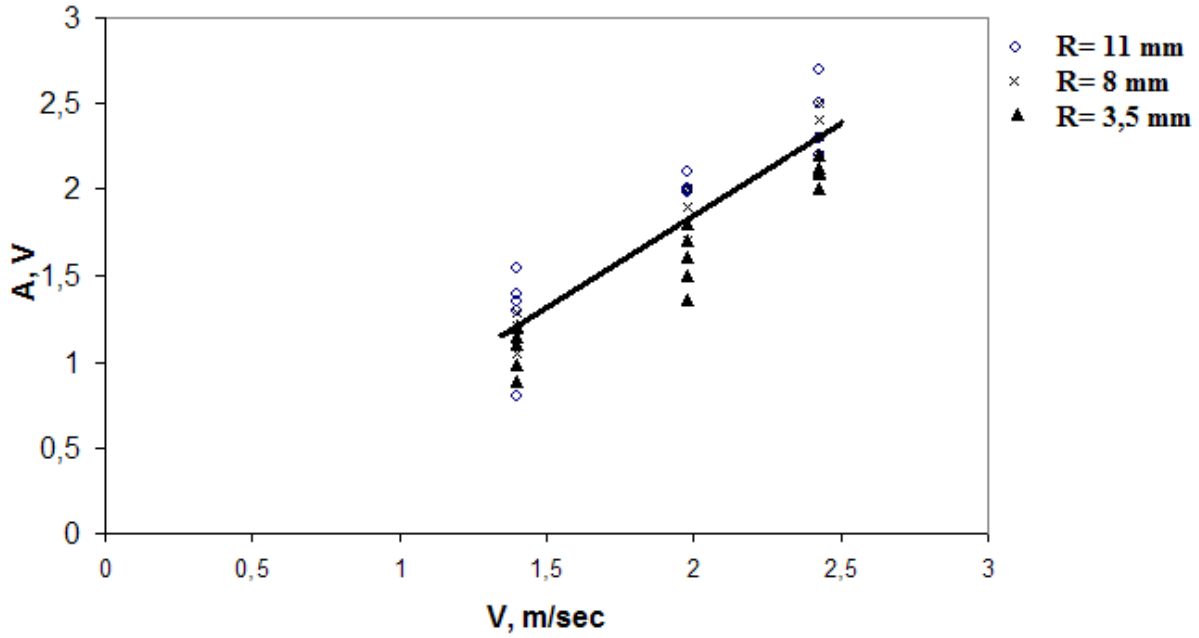

Figure 3. Amplitude – Velocity dependence obtained experimentally for three sphere sizes each dropped from three different heights: 0.1 m, 0.2 m and 0.3 m.

Secondary peaks marked by arrow #2 may be also observed in fig.2 b-e. These peaks relate to unloading of the plate and are separated from the loading related peaks by the delays equal to impact duration. The delay values obtained in more than 10 impacts for every sphere size agree well with the calculated durations of impacts; average durations measured as signal delays and their standard deviations are given in the last columns of the Table 1.

The measured amplitudes of the secondary peaks exceed those of the first peaks and rise from 2.8 V (89 dB) for the small sphere to 8 V (98 dB) for the large one, implying the unloading displacement velocity exceeds the initial loading velocity. Seeming contradiction between the decrease of recoil velocity and the increase of unloading velocity estimated by AE amplitudes may be explained by that velocity is a vector quantity, depending on impact regime. Thus, while at the beginning of loading the impact contact is determined by a normal impulse component only, at the stages of plastic deformation and an unloading, a tangential components occur as well. A change in velocity component orientation leads to the reduction of the algebraic value of the velocity, and hence to the decrease of recoil height.

The above relationships allows one to estimate quantitatively the impact duration and maximum penetration, while a velocity ratio obtained as A_{unld}/A_{ld}, where A_{unld} and A_{ld} are the unloading/ loading related amplitudes of impact waveform, respectively, may serve as an acoustic measure

of energy loss. The higher is the velocity ratio, the greater is the viscoelastic work performed on the materials of the impacting bodies, and therefore the larger is a size of a plastic zone occurring below the contact surface.

3. AE monitoring of cracks

The processes of plastic deformation and crack initiation and growth are considered to be the most important acoustic sources, making a foundation of AE method of nondestructive testing. According to the conclusions of the previous paragraph, AE amplitude from cracking should relate to its rate.

Experimental results we obtained at cyclic loading of reactor steel specimens confirm this statement and give the following relationship between the crack growth and AE amplitude rate and the stress intensity factor [5]:

$$\frac{da}{dN} = C_1(\Delta K_I)^{m_1},$$

$$\frac{dA}{dN} = C_2(\Delta K_I)^{m_2},$$

Where da/dN – is the fatigue crack growth rate; dA/dN – is the summary amplitude rate; $C_{1(2)}$ – are the material constants; $m_{1(2)}$– are the exponents.

The first relationship here is a well known Paris-Erdogan law describing the stage of a steady growth of fatigue crack; the second one is its AE analogue.

From (7a,b) the amplitude – crack growth rate relation was obtained as:

$$\frac{dA}{dN} = C\left(\frac{da}{dN}\right)^m, \text{ where } C = 6 * 10^9; m = 1.59$$

The correlation of mechanic and acoustic parameters is shown fig.4.

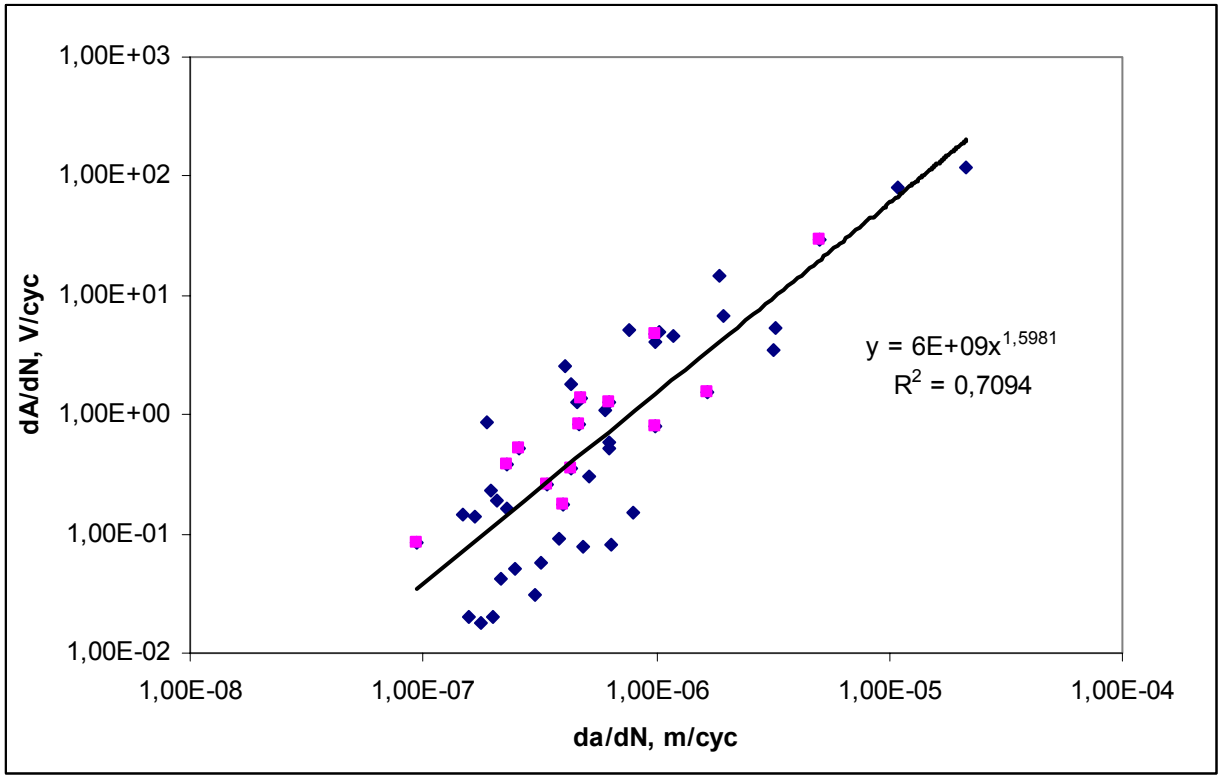

Figure 4. dA/dN *vs* da/dN dependence

The obtained results give a basis for acoustic detection and monitoring of a growing fatigue crack.

To determine AE parameters characterizing level and activity of acoustic emission numerous mechanical testing of carbon and low-alloyed steel specimens were conducted. A temporary dependence of load parameter and acoustic emission amplitude obtained at static loading of 30G2S steel specimens are shown in fig.5. It is seen that the crack jumps are followed by the high amplitude AE signals exceeding the upper limit of the AE apparatus dynamic range. Further special experiments conducted without use of preamplifiers show that a crack jump related amplitude value can exceed 130 dB, i.e. exceed the level of a Shu-Nielsen simulator, which produces amplitudes up to 100 dB.

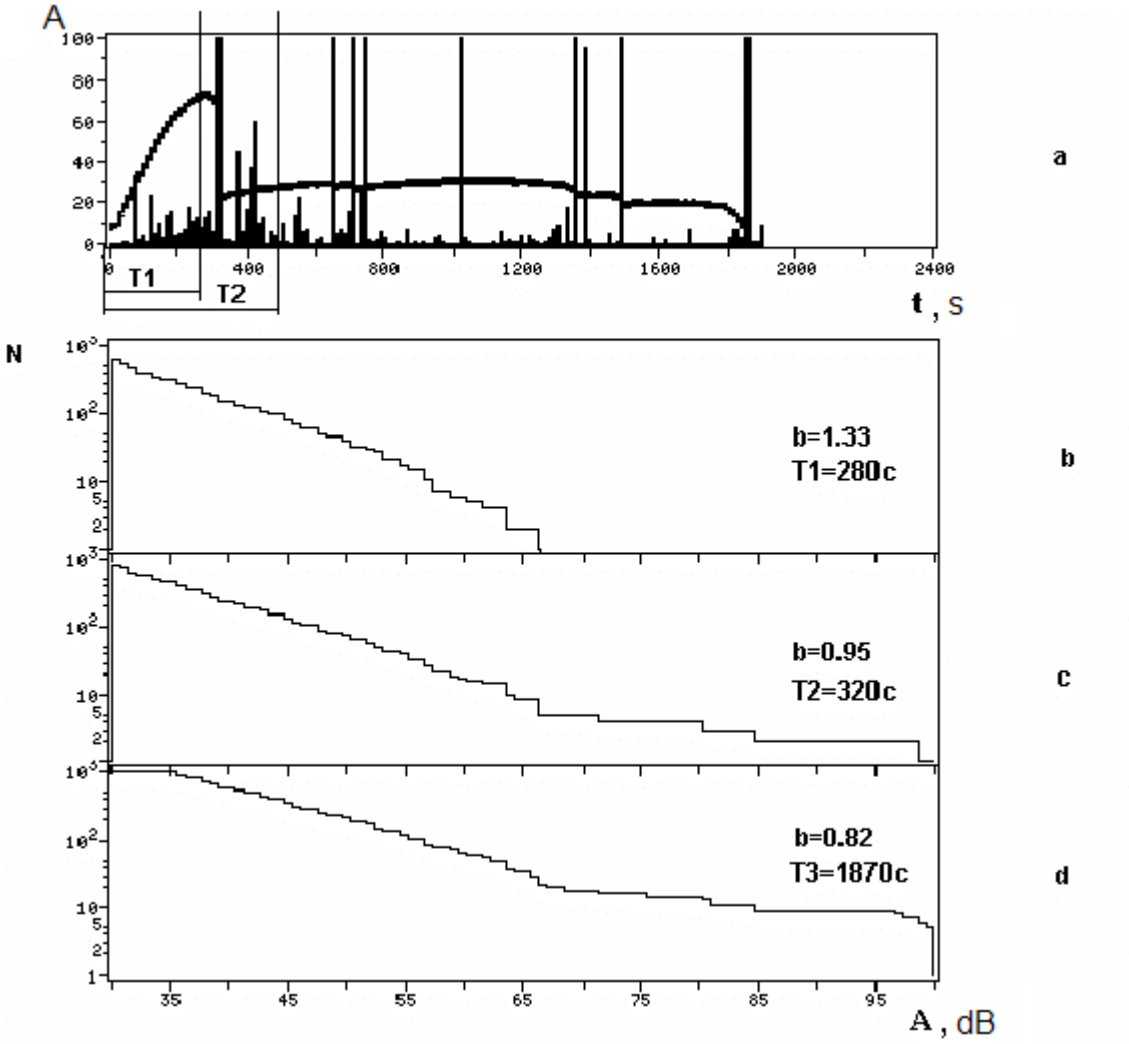

Figure 5. Mechanical loading of a metal specimen. a). Load and AE amplitude temporal dependence. b-d) A-distributions referred to different stages of loading.

To describe a stochastic process of material fracture by means of AE, an amplitude distribution, which is the most informative characteristic giving the level and activity of acoustic emission, is usually studied. Three A-distribution patterns corresponded to different AE sources, namely plastic deformation, microcrack initiation and macro crack growth, are shown in fig.5b-d Based on the results of laboratory testing of metal specimens, the following amplitude ranges are to be assigned to these AE sources:

Table 2 AE amplitudes characterizing fracture mechanisms.

Fracture mechanism	**AE amplitude, dB**
Acts of plastic deformation	A_{th} 50
microcrack initiation	50–80
macro crack growth	80 – 130 and more

These ranges are conditional as they can vary depending on the material characteristics and loading parameters, such as loading deformation rate, material embrittlement, temperature, etc., besides these distributions may overlap. Nevertheless, numeric characteristics of fracture regimes given in the table may serve as basis at the development of AE data processing principles and safety criteria.

Finally, at analysis of AE waveforms from cracking basically the same considerations as at the study of AE from impact may be used. Assume the crack movement function is determined by a broken line function like that given in fig2a. Then a deformation/stress jump will occur at three breakpoints, which are the beginning of crack extension, maximum and crack propagation arrest. The output signals modeled by convolution of input function and a high frequency AE tract response (with range varying from 50 kHz to 200 kHz) are shown in fig. 6b. Each of three signals presented in this figure occurs in the corresponding breakpoint of the crack movement function. They are well distinguished because the intervals between the discontinuity points exceed the decay period. On the contrary, signals in fig.6d overlap and are not separated. Finally, fig.6e,f illustrate the dependence of an output signal amplitude on the value of the derivative jump (velocity jump), which in its turn is determined by the line slopes.

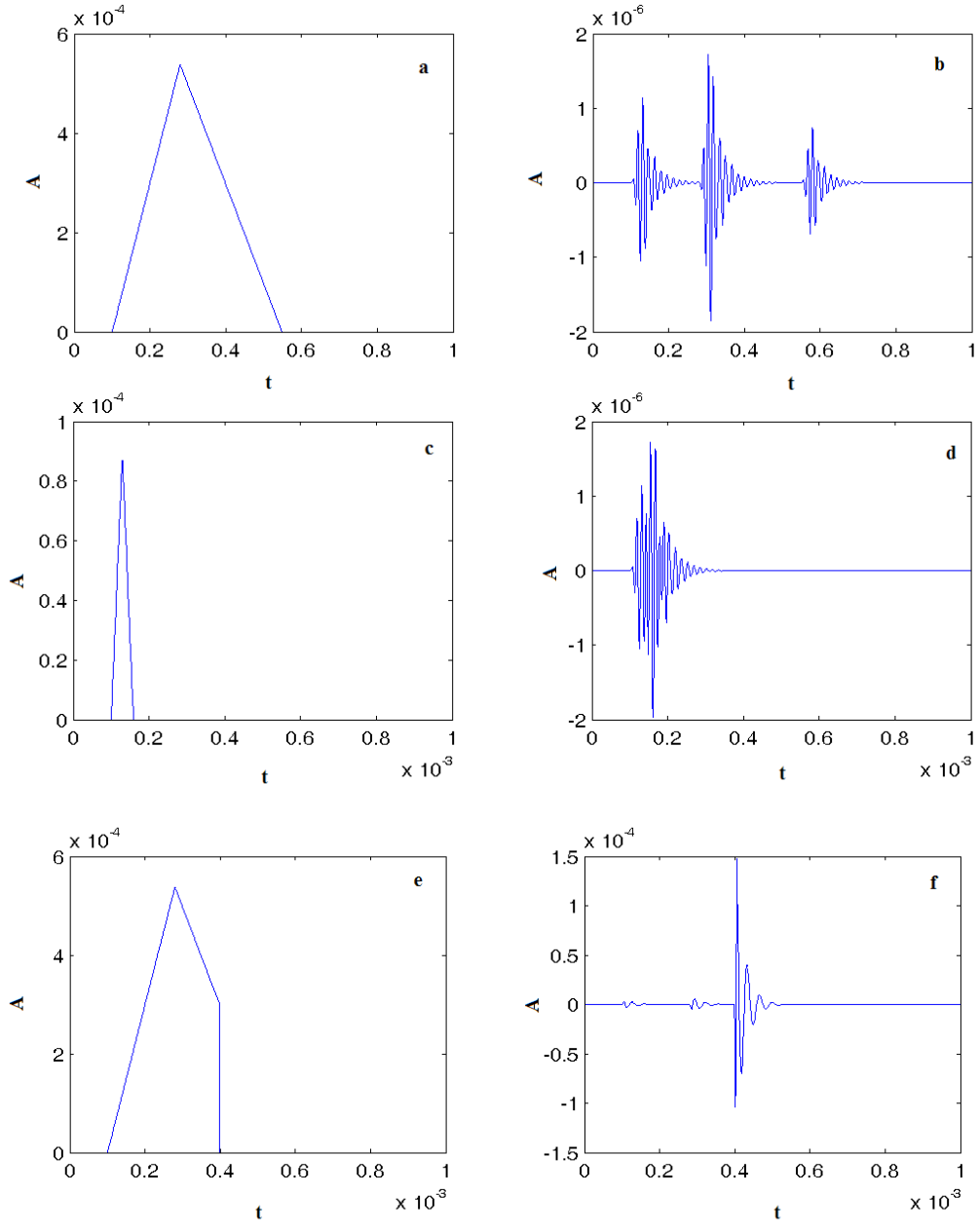

Figure 6. Modeling a high frequency AE crack movement response. (a) The scheme of a slow crack movement function; (b) a modeled output waveform consisting of three signals, which are separated by the time delays corresponding to the breakpoints of the function. (c)The scheme of a rapid crack movement function; (d) a modeled output waveform consisting of overlapping signals; (e, f) dependence of an output signal amplitude on a derivative jump value of input function.

An example of AE waveforms registered by two sensors from cracking of thin Al_2O_3 film is performed in fig.7 . It is look very like the crack's model in fig.6f. The sequence of pulse arrival times and their amplitudes verify these three pulses emitted from the same area, i.e. relate to one crack. In cases when the beginning and the braking moments of a crack movement are distinguished, the crack growth rate may be calculated. In above example for the crack size a = 40mm and the jumping interval Δt = 120 μs the crack rate is equal to 0.33 mm/μs , i.e. it is less by order than a sound speed.

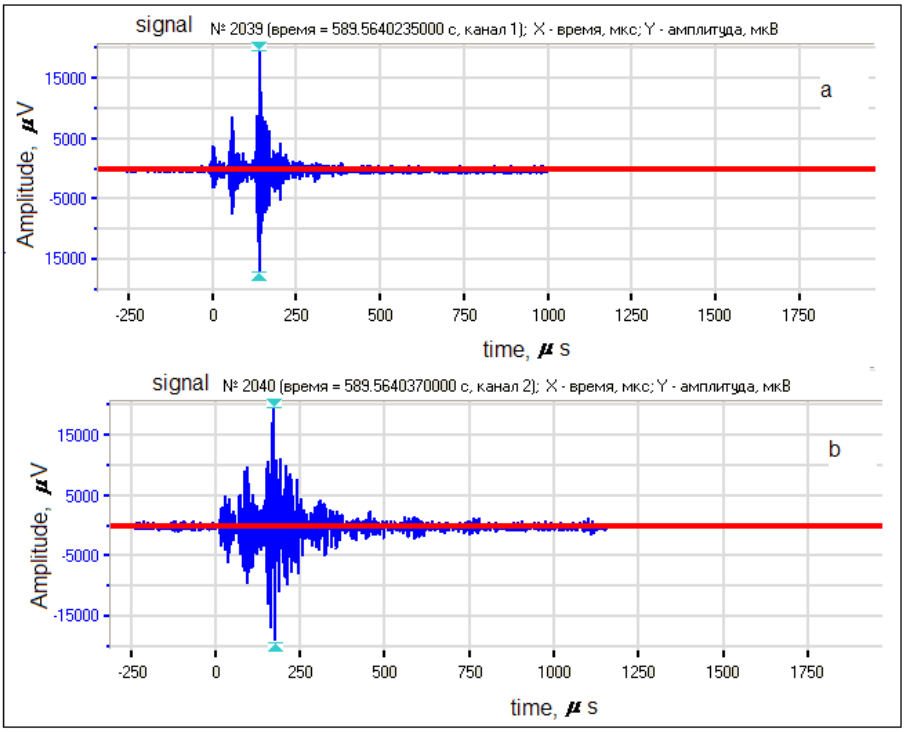

Figure 7. Waveforms registered by two channels. a –sensor with resonance at 500 kHz, b – at 150 kHz

However in most cases the pulses initiated at the beginning and the braking of a crack movement overlap and are not distinguished well.

4. AE leakage detection

Leakage is a continuous process, which may be considered as a broadband stochastic noise. At a low value of a signal to noise ratio, when the temporary-frequency characteristics of the leakage do not differ much from that of a background noise it may be difficult to detect this kind of acoustic source by the standard methods of AE data processing. In this case the problem may be successfully solved by applying a cross correlation method, which is commonly used for detection and location of continuous processes including leakages.

As AE output process from leakage consists of sequences of separate pulses a special correlation algorithm was developed to analyze such discrete data.

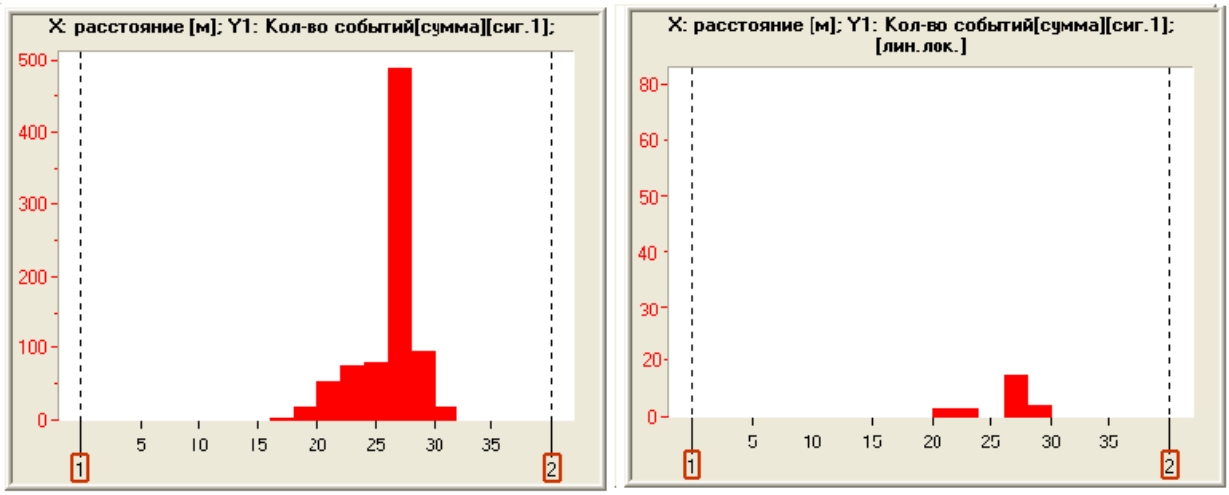

Figure 8. AE events at leakage location: the results of correlation algorithm a) and linear location b)

Fig.8 demonstrates efficiency and advantage of correlation algorithm of hit location over a standard "linear" algorithm.

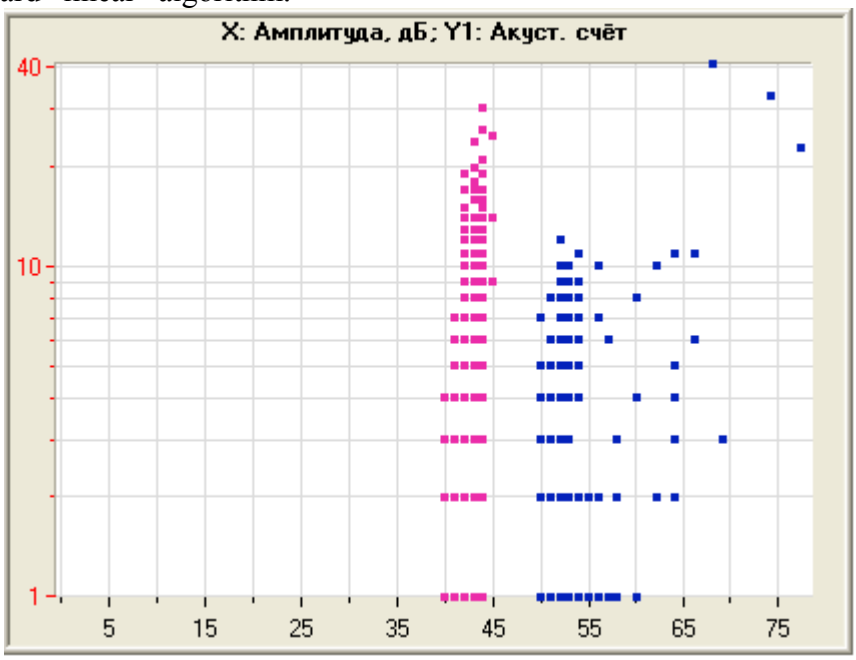

Figure 9. C-A distribution. Nearest channel #2 is blue colored, distant channel #1 is red colored.

C-A plot, see fig.9 gives a typical pattern of distribution, which should be referred to a leakage. Besides, sound attenuation could be easily obtained from these grapics.

Conclusions

1. High frequency AE channel transforms input impact function into two separate signals related first, to loading and second, to unloading of bodies at impact. Signal delay correlate well with the impact duration. Using a double signal effect allows one to estimate the contact time at collision of rigid bodies regardless of the elastic properties and geometry of the bodies, impact direction, etc.
2. An AE amplitude from the impact correlates with the jump in the velocity of the loading function, but not with the function itself. Together with the delay-based measurements of the impact duration, AE amplitude – sphere velocity relationship allows one to estimate the

maximum indentation and the impact force. The ratio of peak amplitudes provides a preliminary evaluation of an impact regime, and therefore, the impact danger.

3. The double signal effect from impacts is observed in different Lamb modes, as well. Signal delays in far zone are equal to that measured in near zone.
4. Theoretical solution for impacts of metal spheres against thick plates allow considering such impacts as calibrated acoustic sources with known parameters along with Shu-Nielsen imitator.
5. The quantitative relations between the fracture mechanic characteristics and the parameters of flow of AE events are performed. AE amplitude distributions refer to different fracture mechanisms are given and a dynamic range of AE corresponding to cracking is discussed.
6. The abilities of AE leakage monitoring and an efficiency of correlation algorithm of location as applied to the discrete flow of AE hits related to leakage is demonstrated and the advantage of this technique over the standard "linear" algorithm of location is shown.

Summarizing the results obtained we conclude that monitoring of the analyzed dynamic sources of damages, traditionally carried out in different frequency ranges by special acoustic techniques may be successfully realized by means of the unique AE method.

Literature

1. Johnson K.L., Contact Mechanics, Cambridge University Press, 1987, 452 p.

2. W.Goldsmith, Impact. E. Arnold Ltd., London,1960

3. Zukas, Jonas A.; Nicholas, T.; Swift, H. F.; Greszczuk, L. B.and Curran, D. R. ,Impact Dynamics, Krieger Publishing Company, Malabar, FL, 1992.

4. H.Deresiewicz. A note on Hertz's theory of impact. Acta Mech.1968, 6,pp. 110–112.

5. Petersen T.B. Processing and interpretation of acoustic emission and electron-microscope data for material damage evaluation. Ph.D. thesis, Moscow,1997, 154 p.